Impurity resonance states in electron-doped high-T_c superconductors

Yuan Wan, Hai-Dong Lü, Hong-Yan Lu, and Qiang-Hua Wang*
National Laboratory of Solid State Microstructures, Department of Physics, Nanjing University, Nanjing 210093, People's Republic of China

(Received 30 September 2007; published 21 February 2008)

Two scenarios, i.e., the anisotropic *s*-wave pairing (the *s*-wave scenario) and the *d*-wave pairing coexisting with antiferromagnetism (the coexisting scenario), have been introduced to understand some of seemingly *s*-wave-like behaviors in electron-doped cuprates. We consider the electronic structure in the presence of a nonmagnetic impurity in the coexistence scenario. We find that even if the antiferromagnetic order opens a full gap in quasiparticle excitation spectra, the midgap resonant peaks in local density of states around an impurity can still be observed in the presence of a *d*-wave pairing gap. The features of the impurity states in the coexisting phase are markedly different from the pure antiferromagnetic or pure *d*-wave pairing phases, showing the unique role of the coexisting antiferromagnetic and *d*-wave pairing orders. On the other hand, it is known that in the pure *s*-wave case, no midgap states can be induced by a nonmagnetic impurity. Therefore, we propose that the response to a nonmagnetic impurity can be used to differentiate the two scenarios.

DOI: 10.1103/PhysRevB.77.064515 PACS number(s): 74.25.Jb, 74.20.−z, 75.50.Ee, 73.43.Jn

I. INTRODUCTION

Up to now, the pairing symmetry of the electron-doped high T_c superconductor is still under debate, and various interpretations for experimental results are controversial. On one hand, the phase-sensitive Josephson junction experiments indicate *d*-wave pairing,[1] and meanwhile angle-resolved photoemission spectra[2] and electronic Raman spectra[3] suggest a nonmonotonic *d*-wave energy gap as a function of momentum. On the other hand, tunneling spectra[4] show more or less *s*-wave-like behavior, i.e., the absence of zero bias conductance peak in the spectrum. Two scenarios have been introduced to explain these results. One is the *s*-wave scenario, in which the *s*-wave character is regarded as the result of anisotropic *s*-wave pairing, but it is incompatible with the phase-sensitive Josephson junction experiment. The other one is the coexisting scenario in which the coexisting antiferromagnetism (AFM) disguises the *d*-wave character of superconductivity (SC).[5,6] The idea of the latter scenario is as follows. First of all, the in-plane AFM has been observed by neutron scattering[7] and transport experiments,[8] and this AFM should be considered naturally. Further, the AFM opens a full gap in single-particle excitation spectrum, which combines with the nodal *d*-wave SC gap to form an effective full single-particle gap. In a recent paper, it is shown that a more careful analysis of the Raman spectra could disentangle the effective gap into its AFM and SC components.[9] It remains to see whether a single-particle probe, such as the scanning tunneling microscopy (STM), could be used to identify the ingredients of the effective gap and hence differentiate the two scenarios. From a theoretical point of view, it is also interesting to unravel the new features in STM in a state with both SC and AFM.

In fact, the impurity in unconventional superconductors proves to be a useful tool to characterize various SC orders. For example, in a *d*-wave superconductor, a zero energy impurity resonant state appears as a hallmark of the *d*-wave pairing symmetry.[10] On the contrary, in conventional *s*-wave superconductor, the resonant state lies at gap edge, which is known as the Yu-Shiba-Rusinov state.[11] The drastic difference is due to the phase structure of the two SC order parameters: in the *d*-wave case, the phase of SC order parameter changes sign across the nodal lines, while in the *s*-wave case, no such sign change occurs. Midgap impurity resonant states can appear in p_x+ip_y and d_x+id_y superconductors as well.[12] Besides, impurity resonant states can also be used to characterize the electronic structure of materials.[13] Furthermore, it is also proposed that inspecting the line shape of the resonant peak as a function of temperature around a nonmagnetic strong impurity can differentiate the phase disorder scenario and *d*-density wave scenario of the pseudogap phase in hole-doped high T_c superconductors.[14] Therefore, STM measurements of the impurity state can provide important messages on the underlying system.[15] The question we now ask is if AFM and *d*-wave SC coexist, what is the nature of the impurity state, and, in particular, whether a low energy resonance state can still arise around the impurity.

In this paper, we calculate the local density of states (LDoS) around a nonmagnetic impurity in the electron-doped high T_c superconductor. Our motivation is to unravel the unique feature in the SC+AFM state, which would help STM to verify or rule out this candidate state. Our main results are as follows. First, although the AFM gap quasiparticles and the bulk density of states (DoS) are *s*-wave-like, two midgap impurity resonant states, lying symmetrically at positive and negative energies, can be observed in the presence of *d*-wave SC. Second, the two resonant peaks in LDoS approach and cross each other when the impurity potential strength increases up to the unitary limit. At an intermediate potential strength, the two peaks merge into one peak at the Fermi energy. Since such midgap impurity resonant states do not appear in the *s*-wave scenario, the two scenarios for the electron-doped high T_c superconductor are differentiable by STM measurements of low energy impurity states. The rest of this paper is arranged as follows. In Sec. II, we describe the model and method. In Sec. III, we present the results. First, we obtained the phase diagram of the system in the absence of impurity. This provides an effective and convenient platform to consider the various phases under concern.

Second, we discuss analytically a toy model with particle-hole symmetry to show the existence of impurity resonance states in the coexisting scenario. Finally, we switch back to the actual situation in the phase diagram and calculate the LDoS in the presence of a nonmagnetic impurity. In order to see the particular role of the AFM and *d*-wave SC coexistence, we compare the actual case to the cases with AFM or *d*-wave SC alone. Section IV is a summary of the work.

II. MODEL AND METHOD

We adopt the t-t'-t''-J model on a square lattice with the Hamiltonian,

$$H = -t\sum_{\langle ij\rangle_1\sigma}(\tilde{c}^{\dagger}_{i\sigma}\tilde{c}_{j\sigma}+\text{H.c.}) - t'\sum_{\langle ij\rangle_2\sigma}(\tilde{c}^{\dagger}_{i\sigma}\tilde{c}_{j\sigma}+\text{H.c.}) - t''\sum_{\langle ij\rangle_3\sigma}(\tilde{c}^{\dagger}_{i\sigma}\tilde{c}_{j\sigma}+\text{H.c.}) + J\sum_{\langle ij\rangle_1}\mathbf{S}_i\cdot\mathbf{S}_j. \quad (1)$$

Here, $\tilde{c}_{i\sigma}$ and $\tilde{c}^{\dagger}_{i\sigma}$ are fermion operators subject to the nondouble-occupancy constraint. $\langle ij\rangle_1$, $\langle ij\rangle_2$, and $\langle ij\rangle_3$ denote the first, second, and third nearest neighbor pairs, respectively. It should be noted that we work in the hole picture, so that a hole in the above model represents a physical electron-double occupancy in electron-doped cuprates. To cope with the above t-J model, we insist in calling the electron-double occupancy as holon unless indicated otherwise. For the parameters, we choose $|t|$ as the unit of energy, so that $t=-1$, $t'=0.32$, $t''=-0.16$, and spin-exchange integral $J=0.3$.[5] We emphasize that the choice of parameters is conventional, and our results are not sensitive to the parameters.

We apply the slave boson mean-field theory (SBMFT), within which the projected fermion operator is decoupled to a spinon and a holon part $\tilde{c}_{i\sigma}=h^{\dagger}_i f_{i\sigma}$, and the restriction of no double occupancy is replaced by the constraint $h^{\dagger}_i h_i+\Sigma_\sigma f^{\dagger}_{i\sigma}f_{i\sigma}=1$.[16] In the mean-field theory, this operator constraint is replaced by its average counterpart. The holon is assumed to condense at zero temperature, so that $h_i, h^{\dagger}_i \to \sqrt{x}$, where x is the doping level. The spin-exchange term is decoupled in a standard way into hopping, pairing, and spin-moment channels,[17]

$$\mathbf{S}_i\cdot\mathbf{S}_j \to -3/8(\langle\hat{\chi}^{\dagger}_{ij}\rangle\hat{\chi}_{ij}+\text{H.c.}) - 3/8(\langle\hat{\Delta}^{\dagger}_{ij}\rangle\hat{\Delta}_{ij}+\text{H.c.}) + (\langle\hat{m}_i\rangle\hat{m}_j+\hat{m}_i\langle m_j\rangle). \quad (2)$$

Here, the bracket $\langle\cdot\rangle$ denotes mean value of an operator. $\hat{\chi}_{ij}=\Sigma_\sigma f^{\dagger}_{i\sigma}f_{j\sigma}$ is the hopping operator, $\hat{\Delta}_{ij}=f_{i\uparrow}f_{j\downarrow}-f_{i\downarrow}f_{j\uparrow}$ is the singlet paring operator, and $\hat{m}_i=1/2\Sigma_\sigma\sigma f^{\dagger}_{i\sigma}f_{i\sigma}$ is the magnetic moment operator. The mean values of these operators are the corresponding order parameters.

We introduce four spinors,

$$\Psi_k=(f_{\mathbf{k}\uparrow},f^{\dagger}_{-\mathbf{k}\downarrow},f_{\mathbf{k}+\mathbf{Q}\uparrow},f^{\dagger}_{-\mathbf{k}-\mathbf{Q}\downarrow})^T,$$

in the momentum space. Here, $\mathbf{Q}=(\pi,\pi)$ is the nesting vector. The mean-field Hamiltonian can be written in terms of the four-spinors as $H^f_{MF}=\bar{\Psi}_{\mathbf{k}}h_{\mathbf{k}}\Psi_{\mathbf{k}}$, where the 4×4 matrix $h_{\mathbf{k}}$ is given by

$$h_{\mathbf{k}}=\begin{pmatrix}\xi_{\mathbf{k}} & \Delta_{\mathbf{k}} & 2Jm & 0\\ \Delta_{\mathbf{k}} & -\xi_{\mathbf{k}} & 0 & 2Jm\\ 2Jm & 0 & \xi_{\mathbf{k}+\mathbf{Q}} & \Delta_{\mathbf{k}+\mathbf{Q}}\\ 0 & 2Jm & \Delta_{\mathbf{k}+\mathbf{Q}} & -\xi_{\mathbf{k}+\mathbf{Q}}\end{pmatrix}. \quad (3)$$

Here, $\xi_{\mathbf{k}}$ is the mean-field dispersion of the fermions, $\Delta_{\mathbf{k}}$ is the paring gap function in momentum space, which are given by

$$\xi_{\mathbf{k}}=-(2xt+3/4J\chi)[\cos(k_x)+\cos(k_y)]-4xt'\cos(k_x)\cos(k_y)-2xt''[\cos(2k_x)+\cos(2k_y)]-\mu,$$

$$\Delta_{\mathbf{k}}=-3/4J\Delta[\cos(k_x)-\cos(k_y)],$$

and m is the staggered magnetic moment. χ is the Hartree-Fock potential, Δ is the pairing potential, and μ is the chemical potential. All of these parameters are obtained through self-consistent mean-field calculation. The spinon's propagator in the above representation is obtained as $\mathcal{G}_{\mathbf{k}}(i\omega_n)=(i\omega_n\mathbf{I}-h_{\mathbf{k}})^{-1}$. The coherent part is given by $\mathcal{G}^{coh}=x\mathcal{G}$ upon convoluting with the holon part.

For later discussion, we define a 2×2 Green's function $G_0(\mathbf{r}_i,\mathbf{r}_j;\tau)=-\hat{T}\langle(f_{i\uparrow},f^{\dagger}_{i\downarrow})^T(\tau)(f^{\dagger}_{j\uparrow},f_{j\downarrow})(0)\rangle$ for the two spinors $(f_{i\uparrow},f^{\dagger}_{i\downarrow})^T$ in the real space and τ is the imaginary time. Its Fourier component in frequency ω_n is related to $\mathcal{G}$ as follows:

$$G_0(\mathbf{r}_i,\mathbf{r}_j;i\omega_n)=\frac{1}{N}\sum_{\mathbf{k}\in MBZ}e^{i\mathbf{k}\cdot(\mathbf{r}_i-\mathbf{r}_j)}[\mathcal{G}_{\mathbf{k},\mathrm{I}}+\mathcal{G}_{\mathbf{k},\mathrm{II}}e^{i\mathbf{Q}\cdot\mathbf{r}_j}+\mathcal{G}_{\mathbf{k},\mathrm{III}}e^{i\mathbf{Q}\cdot\mathbf{r}_i}+\mathcal{G}_{\mathbf{k},\mathrm{IV}}e^{i\mathbf{Q}\cdot(\mathbf{r}_i-\mathbf{r}_j)}], \quad (4)$$

where the summation is over the magnetic Brillouin zone (MBZ) and N is the size of the lattice. The subscripts I, II, III, and IV indicate the left-top, right-top, left-bottom, and right-bottom 2×2 block elements of $\mathcal{G}^{coh}$.

The next step is to obtain the Green function in the presence of a single impurity. We model the impurity by a single-site potential located at the origin and adopt the T-matrix formulation[12,14,18] to calculate the perturbed Green's function G by

$$G(\mathbf{r}_i,\mathbf{r}_j;z)=G_0(\mathbf{r}_i,\mathbf{r}_j;z)+G_0(\mathbf{r}_i,0;z)T(z)G_0(0,\mathbf{r}_j;z), \quad (5)$$

where

$$T(z)=V\sigma_3+V\sigma_3G_0(0,0;z)T(z). \quad (6)$$

Here, z is the complex continuation of $i\omega_n$, V is the nonmagnetic impurity potential, and σ_3 is the third Pauli matrix. In the T-matrix formulation, the correction of mean-field order parameter induced by impurity is ignored. This was shown to be sufficiently consistent with a full self-consistent calculation.[19]

The LDoS can be measured by STM directly, which is given by

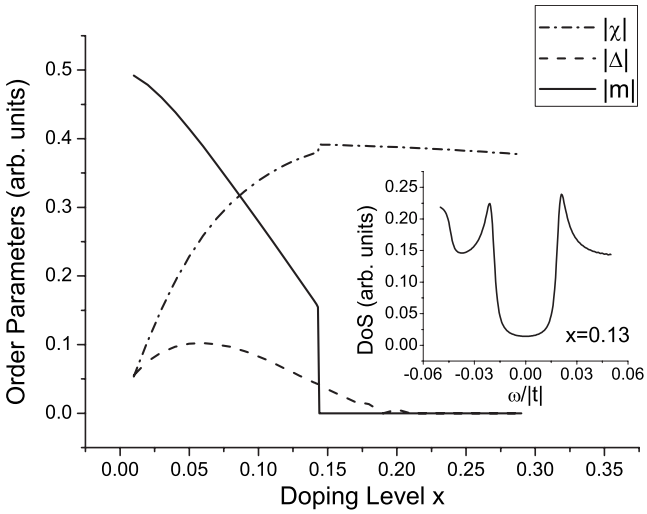

FIG. 1. SBMFT phase diagram of electron-doped superconductor. The dash-dotted line, dashed line, and solid line denote the hopping magnitude, d-wave paring order, and staggered magnetic moment, respectively. The inset shows the bulk density of states at $x=0.13$.

$$\mathcal{N}(\mathbf{r};\omega) = -\frac{1}{\pi}\,\mathrm{Im}[G_{11}(\mathbf{r},\mathbf{r};-\omega+i\eta)+G_{22}(\mathbf{r},\mathbf{r};\omega+i\eta)], \tag{7}$$

where η denotes an infinitely small positive number. The convention of the sign before ω is chosen for the electron-doped case under our concern.

It is perhaps worthwhile to recall that the SBMFT is approximate since it treats the no-double occupancy only on average. As such the theory is often accepted with suspect. We adopt it here for the following reasons. First, our motivation is not to provide an exact solution of the t-J model, which is still a challenge to condensed matter theory. Instead, we use the mean-field theory as an effective framework to capture the debated SC+AFM state. Second, it is clear that the SBMFT is qualitatively equivalent to the renormalized mean-field theory (RMFT) that could be derived from the idea of the Gutzwiller projection under the Gutzwiller approximation.[20] This correspondence suggests that both theories are qualitatively correct. The SBMFT is practically simple and is qualitatively enough for our purpose. Finally, while the incoherent part of the Green function is missing in SBMFT or RMFT, the coherent part is captured and provided qualitatively sensible results.

III. RESULTS

A. Slave boson mean field theory phase diagram

We first present the main results of our SBMFT calculation. The mean-field phase diagram at zero temperature is shown in Fig. 1. The calculation is done on a 1000×1000 lattice. We can see that there are two phase transition points. At $x\approx0.14$, there is a first-order phase transition from the AFM phase to the paramagnetic phase. At $x\approx0.20$, there is a second-order phase transition from the superconducting phase to the normal phase. Thus, in the range of $x<0.14$, the AFM and d-wave SC coexist. The pairing symmetry in this phase is still the standard $d_{x^2-y^2}$ wave. The optimal doping level for the pairing amplitude lies at $x\approx0.06$.

Some remarks are in order here. First, it should be pointed out that pairing itself does not mean superconductivity in a doped Mott insulator. At the mean-field level, a superconducting state requires both pairing and holon condensation. Combining the gauge and thermal phase fluctuations beyond the mean-field level, one could expect a dome-shaped dependence of the superconducting transition temperature T_c as a function of x (with the optimal doping pushed to a higher level), in analogy to the case in the hole-doped cuprates. Since we are considering ground state properties at zero temperature, we do not take these complications into account henceforth. Second, the SC+AFM phase is supported by some neutron[7] and transport[8] experiments. In fact, it was found that at a doping level of $x=0.12$, the in-plane spin-density-wave order is shown to be intrinsic and is enhanced by a c-axis magnetic field that suppresses superconductivity.[7] However, the neutron probe may be affected by the AFM order due to the magnetic ions out of the copper oxide plane. In this sense, considering other probes that would be sensitive to the SC+AFM coexistence is both theoretically interesting and experimentally important. The theoretical results should then be compared to future experimental observations to verify or rule out the candidate state.

Since our main concern is the SC+AFM phase, we plot the local DoS at doping level $x=0.13$ in the inset of Fig. 1. The U-shaped DoS indicates the absence of node in single-particle excitation spectrum, and it has been observed in point contact tunneling spectra but was interpreted as the character of s-wave pairing.[4] In our case, it is a result of coexisting AFM and d-wave SC. The discussed behavior is similar to the one found by Yuan *et al.* within the t-U-V model.[5] We include such a bulk DoS for self-completeness and for comparison with the main results of this paper, i.e., the impurity states.

B. Impurity states in a particle-hole symmetrical case

To see whether resonant impurity states could appear in the coexisting phase, we digress to consider the particle-hole symmetrical case that is analytically tractable. To reach this case, we simply set $\mu=0$, $t'=0$, and $t''=0$. We have $\Delta_{\mathbf{k}}=-\Delta_{\mathbf{k}+\mathbf{Q}}$ and $\xi_{\mathbf{k}}=-\xi_{\mathbf{k}+\mathbf{Q}}$. The unperturbed on-site Green's function $G_0(0,0;z)$ can be calculated explicitly as

$$G_0(0,0;z) = \frac{1}{(2\pi)^2}\int_{BZ} d^2\mathbf{k}\frac{z-b}{z^2-\xi_{\mathbf{k}}^2-\Delta_{\mathbf{k}}^2-b^2}\times\sigma_0. \tag{8}$$

Here, the σ_0 is the 2×2 unit matrix and $b=2Jm$ is the Curie-Weiss potential. The T matrix is given by $T^{-1}(z)=V^{-1}-G^0(0,0;z)$. The position of the resonant state is given by $\det T^{-1}=0$. In the unitary limit $V\to\infty$, the resonance condition is given by $\det G_0(0,0;z)=0$.[12] Since the off-diagonal elements of G_0 is zero due to the d-wave pairing symmetry, the resonance occurs at $z=b$. Since the 11 (or 22) compo-

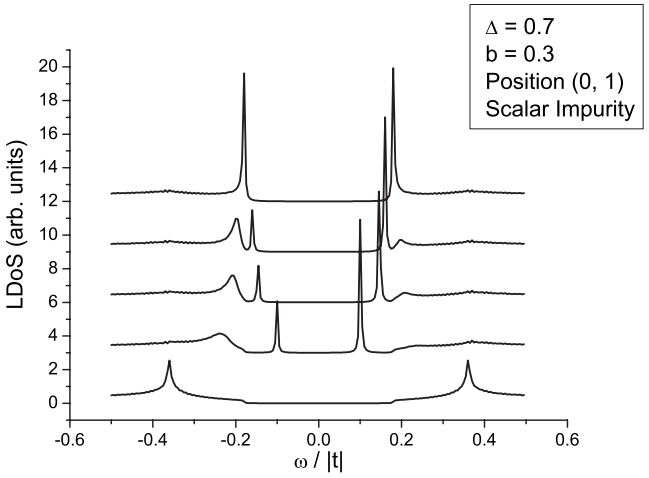

FIG. 2. The dependence of LDoS on impurity potential strength in a particle-hole symmetrical case. From bottom to top, the impurity potential strengths are successively 0, 5, 10, 15, and 1000 in units of $|t|$. Vertical offset is used for clarity.

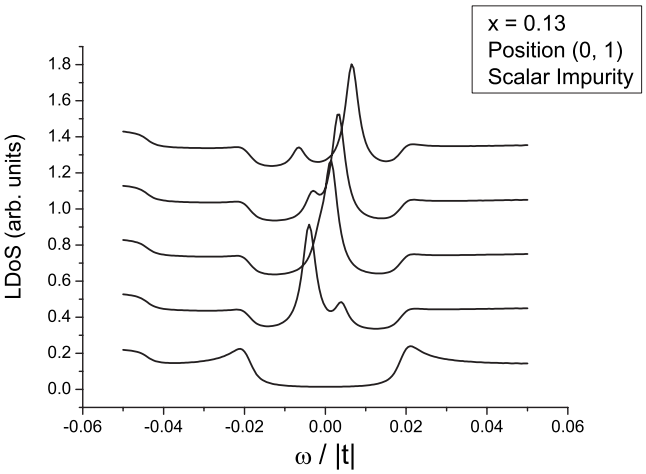

FIG. 3. The dependence of LDoS on impurity scattering strength for actual case. The impurity potential is the same as in Fig. 2.

nents of G describe particles (or holes), we see that another resonance should occur at $z=-b$ in the particle picture alone. This is also evident from the two contributions in the expression for $\mathcal{N}$ in Eq. (7).

If the impurity potential is finite, the situation is more complicated. In Fig. 2, we present the dependence of LDoS on impurity potential strength. In calculation, we simply set $\chi=0$, $\Delta=0.7$, and $b=0.3$ for illustration. The LDoS is for site (0,1), a nearest neighbor of the impurity site. When the potential strength is $V/|t|=5$, there appears already two resonant peaks lying symmetrically at the positive and negative sides. This is different from the particle-hole symmetrical d-wave superconductor, in which only one resonant peak is observed. The doubling of resonant peaks is similar to the one observed in the study of organic superconductivity with bond dimmerization.[21] With increasing potential strength, the resonant peaks shift toward the gap edges, and the height of peaks is strongly enhanced. In the next section, we discuss how the resonance behaves in the realistic situation.

C. Impurity states in electron-doped cuprates

In this section, we discuss the realistic situation in electron-doped cuprates. We choose the result of SBMFT as the input of T-matrix formulation. The evolution of LDoS at site (0,1) with impurity potential strength at the doping level $x=0.13$ is shown in Fig. 3. The mean-field order parameters are $\chi=-0.37$, $\Delta=0.054$, and $m=0.19$. At first, we note that in the unitary limit $V/|t|=1000$, there are two midgap resonant states lying symmetrically at the positive and negative energies, but the heights of the two peaks are different due to the particle-hole asymmetry in the present case. The two peaks are visible for $V/|t|\geqslant 5$. With increasing potential strength, we see that the two peaks seem to cross each other. For $V/|t|=10$, the two peaks meet and merge into one peak which lies right at the Fermi energy. It is therefore clear that resonance states do appear in the coexisting phase, even though the nodal d-wave gap is disrupted by the AFM gap.

D. Pure antiferromagnetism and pure d-wave superconductivity case

In order to understand the unique role of AFM and d-wave SC coexistence, we compare the results in the pure d-wave SC case and the pure AFM case. We set the d-wave SC order parameter to zero in Eq. (3) and leave the AFM order parameter unchanged for pure AFM case. Conversely, we set the AFM order to zero for pure d-wave case. In principle, one should do the self-consistent calculation again in each case. We have done so but found no significant change to the remaining order parameter.

At first, we consider the pure AFM case. The result is shown in Figs. 4(a) and 4(b) for $x=0.06$ and $x=0.13$, respectively. For $x=0.06$, the AFM is strong enough to split the two

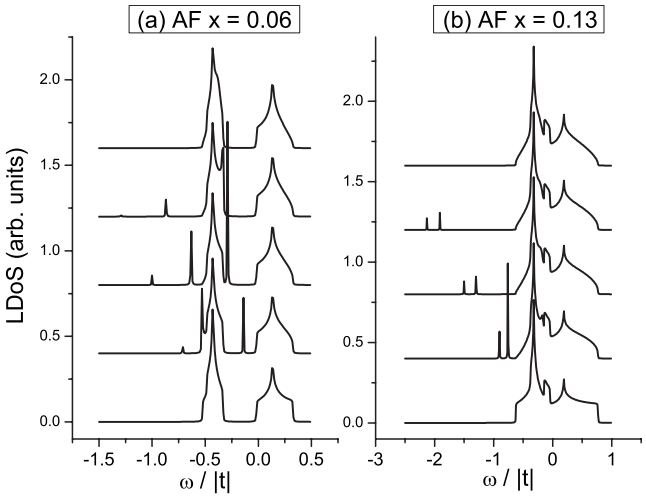

FIG. 4. The impurity state for pure AFM case at two doping levels. The impurity potential is the same as in Fig. 2.

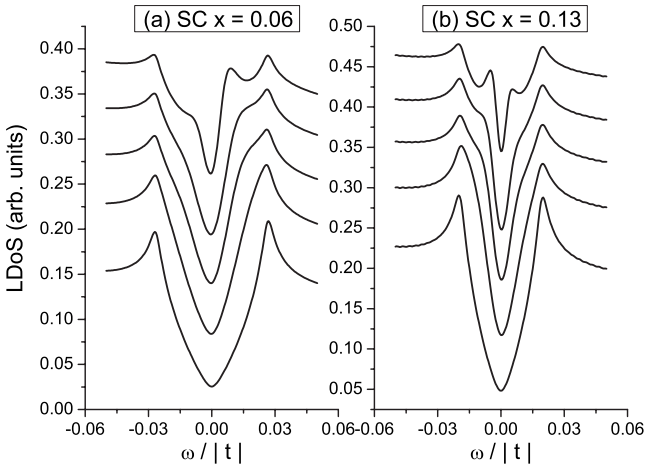

FIG. 5. The impurity state for pure d-wave SC case at two doping levels. The impurity potential is the same as in Fig. 2.

bands, and impurity resonant peaks lie in the gap as well as outside the band. For $x=0.13$, the AFM is weak and the two AFM-induced bands overlap, and then impurity resonant states (the sharp peaks) lie outside bands. The positions of resonant peaks move toward higher energy for higher potential strength and are pushed to infinity in the unitary limit.

Then, we turn to the pure d-wave case shown in Figs. 5(a) and 5(b) for $x=0.06$ and $x=0.13$. We can identify two resonant peaks at the two doping levels, but the strong particle-hole asymmetry has weaken the strength of peaks. On the other hand, the two peaks never cross each other. Moreover, for weak potential strength, these peaks are indiscernible.

Before closing this section, we conclude by comparison that two well-defined midgap resonant peaks appear and cross each other with increasing impurity potential only in the coexisting phase with both AFM and d-wave SC.

IV. SUMMARY

In this work, we discuss the impurity resonant state in the coexisting phase with d-wave SC and AFM. We demonstrate analytically the existence of midgap resonance states in a putative particle-hole symmetrical case and present the results in the realistic case, where the resonance peaks can shift and switch with increasing potential strength. At an intermediate potential strength, the two peaks merge at the Fermi level. These unique features do not appear in the separate pure AFM or pure d-wave SC states. It is also known that midgap impurity states do not appear in a pure s-wave phase. Thus, the impurity state can be used to differentiate the s-wave scenario and the coexisting scenario.

ACKNOWLEDGMENTS

This work was supported by NSFC (Nos. 10325416 and 10734120), the Fok Ying Tung Education Foundation (No. 91009), the Ministry of Science and Technology of China (Grants No. 2006CB921802 and No. 2006CB601002), and the 111 Project (Grant No. B07026).

*qhwang@nju.edu.cn

[1] C. C. Tsuei and J. R. Kirtley, Phys. Rev. Lett. **85**, 182 (2000); Ariando D. Darminto, H. J. H. Smilde, V. Leca, D. H. A. Blank, H. Rogalla, and H. Hilgenkamp, *ibid.* **94**, 167001 (2005).

[2] T. Sato, T. Kamiyama, T. Takahashi, K. Kurahashi, and K. Yamada, Science **291**, 1517 (2001); N. P. Armitage, D. H. Lu, D. L. Feng, C. Kim, A. Damascelli, K. M. Shen, F. Ronning, Z. X. Shen, Y. Onose, Y. Taguchi, and Y. Tokura, Phys. Rev. Lett. **86**, 1126 (2001); H. Matsui, K. Terashima, T. Sato, T. Takahashi, M. Fujita, and K. Yamada, *ibid.* **95**, 017003 (2005); S. R. Park, Y. S. Roh, Y. K. Yoon, C. S. Leem, J. H. Kim, B. J. Kim, H. Koh, H. Eisaki, N. P. Armitage, and C. Kim, Phys. Rev. B **75**, 060501(R) (2007).

[3] G. Blumberg, A. Koitzsch, A. Gozar, B. S. Dennis, C. A. Kendziora, P. Fournier, and R. L. Greene, Phys. Rev. Lett. **88**, 107002 (2002).

[4] S. Kashiwaya, T. Ito, K. Oka, S. Ueno, H. Takashima, M. Koyanagi, Y. Tanaka, and K. Kajimura, Phys. Rev. B **57**, 8680 (1998); A. Biswas, P. Fournier, M. M. Qazilbash, V. N. Smolyaninova, H. Balci, and R. L. Greene, Phys. Rev. Lett. **88**, 207004 (2002); L. Shan, Y. Huang, H. Gao, Y. Wang, S. L. Li, P. C. Dai, F. Zhou, J. W. Xiong, W. X. Ti, and H. H. Wen, Phys. Rev. B **72**, 144506 (2005); L. Shan, Y. Huang, Y. L. Wang, Shiliang Li, Jun Zhao, Pengcheng Dai, Y. Z. Zhang, C. Ren, and H. H. Wen, Phys. Rev. B **77**, 014526 (2008); A. Zimmers, Y. Noat, T. Cren, W. Sacks, D. Roditchev, B. Liang, and R. L. Greene, Phys. Rev. B **76**, 132505 (2007).

[5] Q. S. Yuan, F. Yuan, and C. S. Ting, Phys. Rev. B **73**, 054501 (2006); Q. S. Yuan, X. Z. Yan, and C. S. Ting, *ibid.* **74**, 214503 (2006).

[6] H. G. Luo and T. Xiang, Phys. Rev. Lett. **94**, 027001 (2005); C. S. Liu, H. G. Luo, W. C. Wu, and T. Xiang, Phys. Rev. B **73**, 174517 (2006).

[7] H. J. Kang, P. C. Dai, J. W. Lynn, M. Matsuura, J. R. Thompson, S. C. Zhang, D. N. Argyriouk, Y. Onose, and Y. Tokura, Nature (London) **423**, 522 (2003); H. J. Kang, P. C. Dai, H. A. Mook, D. N. Argyriou, V. Sikolenko, J. W. Lynn, Y. Kurita, S. Komiya, and Y. Ando, Phys. Rev. B **71**, 214512 (2005).

[8] A. N. Lavrov, H. J. Kang, Y. Kurita, T. Suzuki, S. Komiya, J. W. Lynn, S.-H. Lee, P. Dai, and Y. Ando, Phys. Rev. Lett. **92**, 227003 (2004); W. Yu, J. S. Higgins, P. Bach, and R. L. Greene, Phys. Rev. B **76**, 020503 (2007); X. H. Chen, T. Wu, C. H. Wang, G. Wu, D. F. Fang, J. L. Luo, and G. T. Liu, arXiv:0707.0104.

[9] Hong-Yan Lu and Qiang-Hua Wang, Phys. Rev. B **75**, 094502 (2007).

[10] A. V. Balatsky, M. I. Salkola, and A. Rosengren, Phys. Rev. B **51**, 15547 (1995); M. I. Salkola, A. V. Balatsky, and D. J. Scalapino, Phys. Rev. Lett. **77**, 1841 (1996).

[11] L. Yu, Acta Phys. Sin. **21**, 75 (1965); H. Shiba, Prog. Theor. Phys. **40**, 435 (1968); A. I. Rusinov, Sov. Phys. JETP **29**, 1101 (1969).

[12] Q. H. Wang and Z. D. Wang, Phys. Rev. B **69**, 092502 (2004).
[13] T. O. Wehling, A. V. Balatsky, M. I. Katsnelson, A. I. Lichtenstein, K. Scharnberg, and R. Wiesendanger, Phys. Rev. B **75**, 125425 (2007); T. O. Wehling, H. P. Dahal, A. I. Lichtenstein, and A. V. Balatsky, arXiv:0704.3115 (unpublished).
[14] Q. H. Wang, Phys. Rev. Lett. **88**, 057002 (2002).
[15] Ø. Fisher, M. Kugler, I. Maggio-Aprile, C. Berthod, and C. Renner, Rev. Mod. Phys. **79**, 353 (2007).
[16] M. U. Ubbens and P. A. Lee, Phys. Rev. B **46**, 8434 (1992).
[17] J. Brinckmann and P. A. Lee, Phys. Rev. B **65**, 014502 (2001).
[18] A. V. Balatsky, I. Vekhter, and J. X. Zhu, Rev. Mod. Phys. **78**, 373 (2006).
[19] M. Franz, C. Kallin, and A. J. Berlinsky, Phys. Rev. B **54**, R6897 (1996).
[20] D. Vollhardt, Rev. Mod. Phys. **56**, 99 (1984); F. C. Zhang, C. Gros, T. M. Rice, and H. Shiba, Supercond. Sci. Technol. **1**, 36 (1988); Qiang-Hua Wang, Z. D. Wang, Y. Chen, and F. C. Zhang, Phys. Rev. B **73**, 092507 (2006).
[21] Y. Tanuma, K. Kuroki, Y. Tanaka, and S. Kashiwaya, Phys. Rev. B **68**, 214513 (2003).